PHYSICAL REVIEW D **83,** 034002 (2011)

Global analysis of fragmentation functions for eta mesons

Christine A. Aidala[*]
Los Alamos National Laboratory, Los Alamos, New Mexico 87545, USA

Frank Ellinghaus[†]
University of Colorado, Boulder, Colorado 80309, USA
Universität Mainz, Institut für Physik, 55099 Mainz, Germany

Rodolfo Sassot[‡]
Instituto de Física de Buenos Aires, CONICET, Departamento de Física, Facultad de Ciencias Exactas y Naturales, Universidad de Buenos Aires, Ciudad Universitaria, Pabellón 1 (1428) Buenos Aires, Argentina

Joseph P. Seele[§]
University of Colorado, Boulder, Colorado 80309, USA
Massachusetts Institute of Technology, Cambridge, Massachusetts 02139-4307, USA

Marco Stratmann[‖]
Institut für Theoretische Physik, Universität Regensburg, 93040 Regensburg, Germany
(Received 5 October 2010; published 1 February 2011)

Fragmentation functions for eta mesons are extracted at next-to-leading order accuracy of QCD in a global analysis of data taken in electron-positron annihilation and proton-proton scattering experiments. The obtained parametrization is in good agreement with all data sets analyzed and can be utilized, for instance, in future studies of double-spin asymmetries for single-inclusive eta production. The Lagrange multiplier technique is used to estimate the uncertainties of the fragmentation functions and to assess the role of the different data sets in constraining them.

DOI: 10.1103/PhysRevD.83.034002 PACS numbers: 13.87.Fh, 12.38.Bx, 13.85.Ni

I. INTRODUCTION

Fragmentation functions (FFs) are a key ingredient in the perturbative QCD (pQCD) description of processes with an observed hadron in the final state. Similar to parton distribution functions (PDFs), which account for the universal partonic structure of the interacting hadrons, FFs encode the nonperturbative details of the hadronization process [1]. When combined with the perturbatively calculable hard scattering cross sections, FFs extend the ideas of factorization to a much wider class of processes ranging from hadron production in electron-positron annihilation to semi-inclusive deep-inelastic scattering (SIDIS) and hadron-hadron collisions [2].

Over the last years, our knowledge on FFs has improved dramatically [3] from first rough models of quark and gluon hadronization probabilities [4] to rather precise global analyses at next-to-leading order (NLO) accuracy of QCD, including estimates of uncertainties [5–8]. While the most accurate and clean information used to determine FFs comes from single-inclusive electron-positron annihilation (SIA) into hadrons, such data do not allow disentanglement of quark from antiquark fragmentation and constrain the gluon fragmentation only weakly through scaling violations and subleading NLO corrections. Modern global QCD analyses [5,6] utilize to the extent possible complementary measurements of hadron spectra obtained in SIDIS and hadron-hadron collisions to circumvent these shortcomings and to constrain FFs for all parton flavors individually.

Besides the remarkable success of the pQCD approach in describing all the available data simultaneously, the picture emerging from such comprehensive studies reveals interesting and sometimes unexpected patterns between the FFs for different final-state hadrons. For instance, the strangeness-to-kaon fragmentation function obtained in Ref. [5] is considerably larger than those assumed previously in analyses of SIA data alone [9]. This has a considerable impact on the extraction of the amount of strangeness polarization in the nucleon [10] from SIDIS data, which in turn is linked to the fundamental question of how the spin of the nucleon is composed of intrinsic spins and orbital angular momenta of quarks and gluons.

Current analyses of FFs comprise pions, kaons, protons [5–8], and lambdas [7,11] as final-state hadrons. In this respect, FFs are a much more versatile tool to explore nonperturbative aspects of QCD than PDFs where studies

[*]caidala@bnl.gov
[†]ellingha@uni-mainz.de
[‡]sassot@df.uba.ar
[§]seelej@mit.edu
[‖]Present address: Physics Department, Brookhaven National Laboratory, Upton, NY 11973, USA.
marco@ribf.riken.jp

are mainly restricted to protons [12,13]. In the following, we extend the global QCD analyses of FFs at NLO accuracy as described in Refs. [5,6] to eta mesons and estimate the respective uncertainties with the Lagrange multiplier method [5,10,14]. We obtain a parametrization from experimental data for single-inclusive eta meson production in SIA at various center-of-mass system (c.m.s.) energies $\sqrt{S}$ and proton-proton collisions at the Brookhaven National Laboratory Relativistic Heavy Ion Collider (RHIC) in a wide range of transverse momenta p_T. We note two earlier determinations of eta FFs in Refs. [15,16] which are based on normalizations taken from a Monte Carlo event generator and $SU(3)$ model estimates, respectively. In both cases, parametrizations are not available.

The newly obtained FFs provide fresh insight into the hadronization process by comparing to FFs for other hadrons. In particular, the peculiar wave function of the eta, $|\eta\rangle \simeq |u\bar{u} + d\bar{d} - 2s\bar{s}\rangle$, with all light quarks and antiquarks being present, may reveal new patterns between FFs for different partons and hadrons. The similar mass range of kaons and etas, $m_{K^0} \simeq 497.6$ MeV and $m_\eta \simeq 547.9$ MeV, respectively, and the presence of strange quarks in both wave functions make comparisons between the FFs for these mesons especially relevant. Of specific interest is also the apparently universal ratio of eta to neutral pion yields for $p_T \gtrsim 2$ GeV in hadron-hadron collisions across a wide range of c.m.s. energies (see, e.g., Ref. [17]) and how this is compatible with the extracted eta and pion FFs.

In addition, the availability of eta FFs permits for the first time NLO pQCD calculations of double-spin asymmetries for single-inclusive eta meson production at high p_T which have been measured at RHIC [18] recently. Such calculations are of topical interest for global QCD analyses of the spin structure of the nucleon [10]. Finally, the set of eta FFs also provides the baseline for studies of possible modifications in a nuclear medium [19,20], for instance, in deuteron-gold collisions at RHIC [17].

The remainder of the paper is organized as follows: Next, we give a brief outline of the analysis. In Sec. III we present the results for the eta FFs, compare to data, and discuss our estimates of uncertainties. We conclude in Sec. IV.

II. OUTLINE OF THE ANALYSIS

A. Technical framework and parametrization

The pQCD framework at NLO accuracy for the scale evolution of FFs [21] and single-inclusive hadron production cross sections in SIA [22] and hadron-hadron collisions [23] has been in place for quite some time and does not need to be repeated here. Likewise, the global QCD analysis of the eta FFs itself follows closely the methods outlined in a corresponding fit of pion and kaon FFs in Ref. [5], where all the details can be found. As in [5,6] we use the Mellin technique as described in [10,24] to implement all NLO expressions. Here, we highlight the differences to similar analyses of pion and kaon FFs and discuss their consequences for our choice of the functional form parameterizing the FFs of the eta meson.

As compared to lighter hadrons, in particular, pions, data with identified eta mesons are less abundant and less precise. Most noticeable is the lack of any experimental information from SIDIS so far, which provided the most important constraints on the separation of contributions from u, d, and s (anti)quarks fragmenting into pions and kaons [5]. Since no flavor-tagged data exist for SIA either, it is inevitable that a fit for eta FFs has considerably less discriminating power. Hence, instead of extracting the FFs for the light quarks and antiquarks individually, we parametrize the flavor singlet combination at an input scale of $\mu_0 = 1$ GeV, assuming that all FFs are equal, i.e., $D_u^\eta = D_{\bar{u}}^\eta = D_d^\eta = D_{\bar{d}}^\eta = D_s^\eta = D_{\bar{s}}^\eta$. We use the same flexible functional form as in Ref. [5] with five fit parameters:

$$D_i^\eta(z,\mu_0) = N_i z^{\alpha_i}(1-z)^{\beta_i}[1+\gamma_i(1-z)^{\delta_i}] \times \frac{1}{B[2+\alpha_i,\beta_i+1]+\gamma_i B[2+\alpha_i,\beta_i+\delta_i+1]}, \quad (1)$$

where z is the fraction of the four-momentum of the parton taken by the eta meson and $i = u, \bar{u}, d, \bar{d}, s, \bar{s}$. $B[a,b]$ denotes the Euler beta function with a and b chosen such that N_i is normalized to the second moment $\int_0^1 z D_i^\eta(z,\mu_0)dz$ of the FFs.

Although the assumption of equal light quark FFs seems to be rather restrictive at first, such an ansatz can be anticipated in view of the wave function of the eta meson. One might expect a difference between strange and nonstrange FFs though due to the larger mass of strange quarks, i.e., that the hadronization of u or d quarks is somewhat less likely as they need to pick up an $s\bar{s}$ pair from the vacuum to form the eta. Indeed, a "strangeness suppression" is found for kaon FFs [5] leading, for instance, to $D_s^{K^-} > D_{\bar{u}}^{K^-}$. In the case of the eta wave function one can argue, however, that also a fragmenting s quark needs to pick up an $s\bar{s}$ pair from the vacuum. Nevertheless, we have explicitly checked that the introduction of a second independent parameterization like in (1) to discriminate between the strange and nonstrange FFs does not improve the quality of the fit to the currently available data. Clearly, SIDIS data would be required to further refine our assumptions in the light quark sector in the future.

The gluon-to-eta fragmentation D_g^η is mainly constrained by data from RHIC rather than scaling violations in SIA. As for pion and kaon FFs in [5], we find that a simplified functional form with $\gamma_g = 0$ in Eq. (1) provides enough flexibility to accommodate all data.

Turning to the fragmentation of heavy charm and bottom quarks into eta mesons, we face the problem that none of the available data sets constrains their contributions significantly. Here, the lack of any flavor-tagged data from SIA hurts most as hadron-hadron cross sections at RHIC energies do not receive any noticeable contributions from heavy quark fragmentation. Introducing independent FFs for charm and bottom at their respective mass thresholds improves the overall quality of the fit but their parameters are essentially unconstrained. For this reason, we checked that taking the shape of the much better constrained charm and bottom FFs for pions, kaons, protons, and residual charged hadrons from [5,6], but allowing for different normalizations, leads to fits of comparable quality with only two additional free parameters.

The best fit is obtained for the charm and bottom FFs from an analysis of residual charged hadrons [6], i.e., hadrons other than pions, kaons, and protons, and hence we use

$$\begin{aligned} D_c^\eta(z,m_c) &= D_{\bar{c}}^\eta(z,m_c) = N_c D_c^{\mathrm{res}}(z,m_c), \\ D_b^\eta(z,m_b) &= D_{\bar{b}}^\eta(z,m_b) = N_b D_b^{\mathrm{res}}(z,m_b). \end{aligned} \tag{2}$$

N_c and N_b denote the normalizations for the charm and bottom fragmentation probabilities at their respective initial scales, to be constrained by the fit to data. The parameters specifying the $D_{c,b}^{\mathrm{res}}$ can be found in Table III of Ref. [6]. The FFs in Eq. (2) are included discontinuously as massless partons in the scale evolution of the FFs above their $\overline{\mathrm{MS}}$ thresholds $\mu = m_{c,b}$ with $m_c = 1.43$ GeV and $m_b = 4.3$ GeV denoting the mass of the charm and bottom quark, respectively.

In total, the parameters introduced in Eqs. (1) and (2) to describe the FFs of quarks and gluons into eta mesons add up to 10. They are determined by a standard χ^2 minimization for $N = 140$ data points, where

$$\chi^2 = \sum_{j=1}^{N} \frac{(T_j - E_j)^2}{\delta E_j^2}. \tag{3}$$

E_j represents the experimentally measured value of a given observable, δE_j is its associated uncertainty, and T_j is the corresponding theoretical estimate calculated at NLO accuracy for a given set of parameters in Eqs. (1) and (2). For the experimental uncertainties δE_i we take the statistical and systematic errors in quadrature for the time being.

B. Data sets included in the fit

A total of 15 data sets is included in our analysis. We use all SIA data with $\sqrt{S} > 10$ GeV: HRS [25] and MARK-II [26] at $\sqrt{S} = 29$ GeV, JADE [27,28] and CELLO [29] at $\sqrt{S} = 34$–35 GeV, and ALEPH [30–32], L3 [33,34], and OPAL [35] at $\sqrt{S} = M_Z = 91.2$ GeV. Preliminary results from *BABAR* [36] at $\sqrt{S} = 10.54$ GeV are also taken into account.

The availability of e^+e^- data in approximately three different energy regions of $\sqrt{S} \simeq 10$, 30, and 90 GeV helps to constrain the gluon fragmentation function from scaling violations. Also, the appropriate electroweak charges in the inclusive process $e^+e^- \to (\gamma, Z) \to \eta X$ vary with energy (see, e.g., Appendix A of Ref. [11] for details) and hence control which combinations of quark FFs are probed. Only the CERN-LEP data taken on the Z resonance receive significant contributions from charm and bottom FFs.

Given that the range of applicability for FFs is limited to medium-to-large values of the energy fraction z, as discussed, e.g., in Ref. [5], data points with $z < 0.1$ are excluded from the fit. Whenever the data set is expressed in terms of the scaled three-momentum of the eta meson, i.e., $x_p \equiv 2p_\eta/\sqrt{S}$, we convert it to the usual scaling variable $z = x_p/\beta$, where $\beta = p_\eta/E_\eta = \sqrt{1 - m_\eta^2/E_\eta^2}$. In addition to the cut $z > 0.1$, we also impose that $\beta > 0.9$ in order to avoid kinematic regions where mass effects become increasingly relevant. The cut on β mainly affects the data at low z from *BABAR* [36].

In case of single-inclusive eta meson production in hadron-hadron collisions, we include data sets from PHENIX at $\sqrt{S} = 200$ GeV at midrapidity [17,18] in our global analysis. The overall scale uncertainty of 9.7% in the PHENIX measurement is not included in δE_j in Eq. (3). All data points have a transverse momentum p_T of at least 2 GeV. As we shall demonstrate below, these data provide an invaluable constraint on the quark and gluon-to-eta fragmentation probabilities. In general, hadron collision data probe FFs at fairly large momentum fractions $z \gtrsim 0.5$; see, e.g., Fig. 6 in Ref. [37], complementing the information available from SIA. The large range of p_T values covered by the recent PHENIX data [18], $2 \le p_T \le 20$ GeV, also helps to constrain FFs through scaling violations.

As in other analyses of FFs [5,6] we do not include eta meson production data from hadron-hadron collision experiments at much lower c.m.s. energies, like Fermilab-E706 [38]. It is known that theoretical calculations at NLO accuracy do not reproduce such data very well without invoking resummations of threshold logarithms to all orders in pQCD [39].

III. RESULTS

In this section we discuss in detail the results of our global analysis of FFs for eta mesons at NLO accuracy of QCD. First, we shall present the parameters of the optimum fits describing the D_i^η at the input scale. Next, we compare our fits to the data used in the analysis and give χ^2 values for each individual set of data. Finally, we estimate the uncertainties in the extraction of the D_i^η using the Lagrange multiplier technique and discuss the role of the different data sets in constraining the FFs.

TABLE I. Parameters describing the NLO FFs for eta mesons, $D_i^\eta(z, \mu_0)$, in Eqs. (1) and (2) at the input scale $\mu_0 = 1$ GeV. Inputs for the charm and bottom FFs refer to $\mu_0 = m_c$ and $\mu_0 = m_b$, respectively.

Flavor i	N_i	α_i	β_i	γ_i	δ_i
$u, \bar{u}, d, \bar{d}, s, \bar{s}$	0.038	1.372	1.487	2000.0	34.03
g	0.070	10.00	9.260	0	0
$c, \bar{c}$	1.051	...	...	...	...
$b, \bar{b}$	0.664	...	...	...	...

A. Optimum fit to data

In Table I we list the set of parameters specifying the optimum fit of eta FFs at NLO accuracy in Eqs. (1) and (2) at our input scale $\mu_0 = 1$ GeV for the light quark flavors and the gluon. Charm and bottom FFs are included at their mass threshold $\mu_0 = m_c$ and $\mu_0 = m_b$, respectively [40].

The data sets included in our global analysis, as discussed in Sec. II B, and the individual χ^2 values are presented in Table II. We note that the quoted numbers of points and χ^2 values are based only on fitted data, i.e., $z > 0.1$ and $\beta > 0.9$ in SIA.

As can be seen, for most sets of data their partial contribution to the χ^2 of the fit is typically of the order of the number of data points or even smaller. The most notable exceptions are the HRS [25] and ALEPH '02 [32] data, where a relatively small number of points have a significant χ^2, which in turn leads to total χ^2 per degree of freedom of about 1.6 for the fit. We have checked that these more problematic sets of data could be removed from the fit without reducing its constraining power or changing the obtained D_i^η significantly. The resulting, fairly large χ^2/degree of freedom due to a few isolated data points is a common characteristic of all extractions of FFs made so far [5–9] for other hadron species.

TABLE II. Data used in the global analysis of eta FFs, the individual χ^2 values for each set, and the total χ^2 of the fit.

Experiment	Data points fitted	χ^2
BABAR [36]	18	8.1
HRS [25]	13	51.6
MARK-II [26]	7	3.8
JADE '85 [27]	1	9.6
JADE '90 [28]	3	1.2
CELLO [29]	4	1.1
ALEPH '92 [30]	8	2.0
ALEPH '00 [31]	18	22.0
ALEPH '02 [32]	5	61.6
L3 '92 [33]	3	5.1
L3 '94 [34]	8	10.5
OPAL [35]	9	9.0
PHENIX 2γ [17]	12	4.1
PHENIX 3π [17]	6	2.9
PHENIX '06 [18]	25	13.3
TOTAL	140	205.9

The overall excellent agreement of our fit with experimental results for inclusive eta meson production in SIA and the tension with the HRS and ALEPH '02 data is also illustrated in Fig. 1. It is worth pointing out that both ALEPH '00 [31] and *BABAR* [36] data are well reproduced for all momentum fractions z in spite of being at opposite ends of the c.m.s. energy range covered by experiments.

Our fit compares very well with all data on high-p_T eta meson production in proton-proton collisions from RHIC [17,18]. The latest set of PHENIX data [18] significantly extends the range in p_T at much reduced uncertainties and provides stringent constraints on the FFs as we shall demonstrate below. The normalization and trend of the data are nicely reproduced over a wide kinematical range as can be inferred from Figs. 2–4. In each case, the invariant cross section for $pp \to \eta X$ at $\sqrt{S} = 200$ GeV is computed at NLO accuracy, averaged over the pseudorapidity range of PHENIX, $|\eta| \leq 0.35$, and using the NLO set of PDFs from CTEQ [12] along with the corresponding value of α_s. Throughout our analysis we choose the transverse momentum of the produced eta as both the factorization and the renormalization scales, i.e., $\mu_f = \mu_r = p_T$.

Since the cross sections drop over several orders of magnitude in the given range of p_T, we show also the ratio (data-theory)/theory in the lower panels of Figs. 2–4 to facilitate the comparison between the data and our fit. One notices the trend of the theoretical estimates to overshoot the data near the lowest values of transverse momenta, $p_T \simeq 2$ GeV, which indicates that the factorized pQCD approach starts to fail. Compared to pion production at central pseudorapidities (see Fig. 6 in Ref. [5]), the breakdown of pQCD sets in at somewhat higher p_T as is expected due to the larger mass of the eta meson.

The shaded bands in Figs. 2–4 are obtained with the Lagrange multiplier method [see Sec. III B below] applied to each data point. They correspond to the maximum variation of the invariant cross section computed with alternative sets of eta FFs consistent with an increase of $\Delta\chi^2 = 1$ or $\Delta\chi^2 = 2\%$ in the total χ^2 of the best global fit to all SIA and pp data.

In addition to the experimental uncertainties propagated to the extracted D_i^η, a large theoretical ambiguity is associated with the choice of the factorization and renormalization scales used in the calculation of the $pp \to \eta X$ cross sections. These uncertainties are usually not accounted for in global fits of PDFs [12,13] and FFs [5–8]. For the most recent PHENIX data, scale uncertainties are more sizable than experimental ones, even at NLO accuracy, in the low to medium p_T range (see Fig. 2 of Ref. [18]) and similar to those estimated for $pp \to \pi X$ in Fig. 6 of Ref. [5]. Following the de Florian-Sassot-Stratmann (DSS) analysis for pion and kaon FFs [5], the choice $\mu_f = \mu_r = p_T$ and $\mu_f = \mu_r = S$ in pp collisions and SIA, respectively, leads

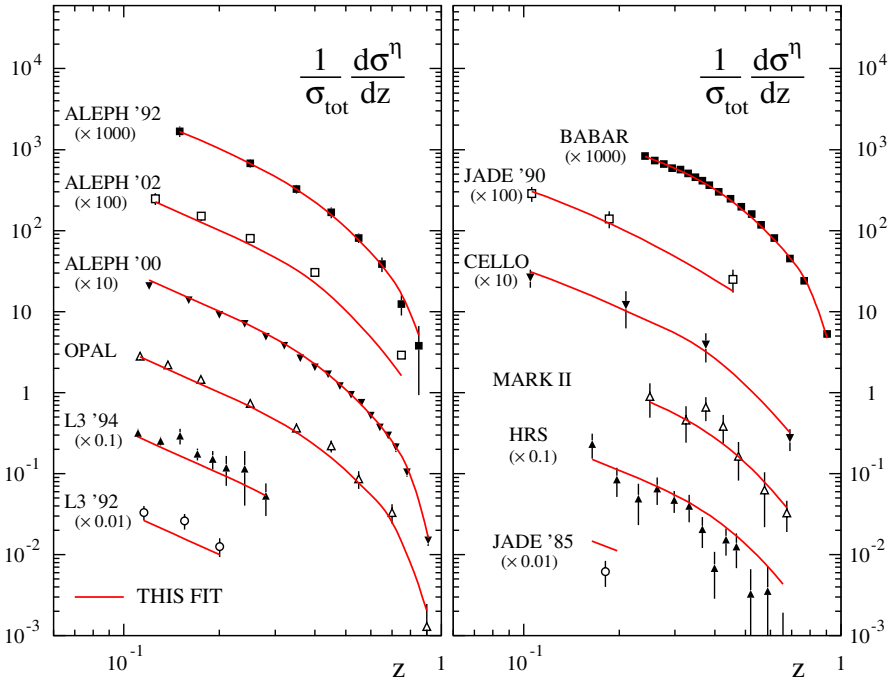

FIG. 1 (color online). Comparison of our NLO results with the data sets for inclusive eta meson production in SIA used in the fit; see Table II.

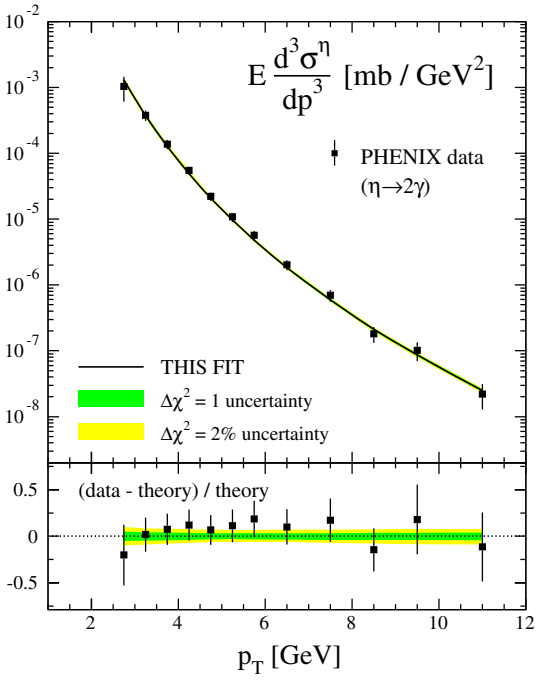

FIG. 2 (color online). Upper panel: Comparison of our NLO result for single-inclusive eta production in pp collisions at $\sqrt{S} = 200$ GeV with PHENIX data where the eta is identified in the decay $\eta \to 2\gamma$ [17]. Lower panel: The ratio (data-theory)/theory. The shaded bands correspond to alternative fits consistent with an increase of $\Delta\chi^2 = 1$ or $\Delta\chi^2 = 2\%$ in the total χ^2 of the best fit (see the text).

to a nice global description of all data sets with a common universal set of eta FFs. As usual, estimates of uncertainties for the D_i^η below refer to a fixed set of scales and are expected to be similar for any given choice of scales. Ultimately, higher order corrections beyond NLO

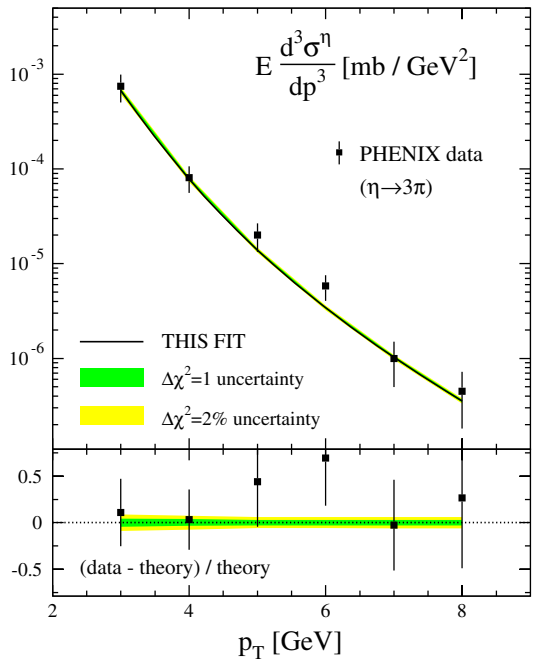

FIG. 3 (color online). The same as in Fig. 2 but now for the data where the eta is identified in the decay $\eta \to 3\pi$ [17].

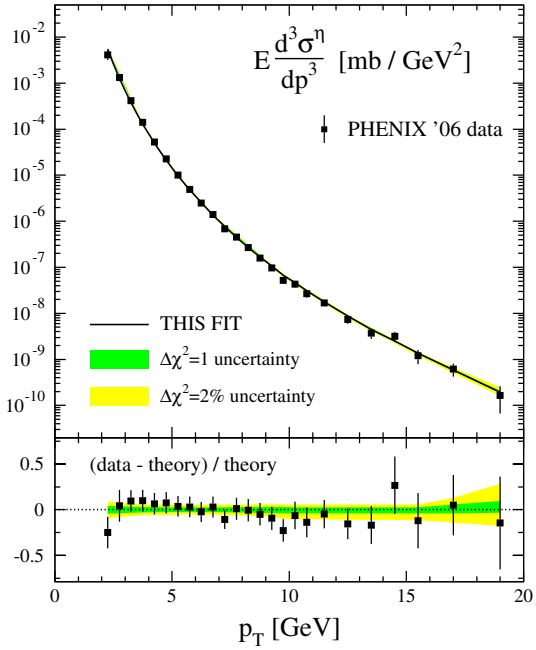

FIG. 4 (color online). The same as in Fig. 2 but now for the latest PHENIX data [18].

accuracy, which have not been computed yet, will reduce the theoretical scale uncertainties.

Next, we shall present an overview of the obtained FFs $D_i^\eta(z, Q)$ for different parton flavors i and compare them to FFs for other hadrons. The upper row of panels in Fig. 5 shows the dependence of the FFs on the energy fraction z taken by the eta meson at a scale Q equal to the mass of the Z boson, i.e., $Q = M_Z$. Recall that at our input scale $Q = \mu_0 = 1$ GeV we assume that $D_u^\eta = D_{\bar{u}}^\eta = D_d^\eta = D_{\bar{d}}^\eta = D_s^\eta = D_{\bar{s}}^\eta$, which is preserved under scale evolution. At such a large scale $Q = M_Z$ the heavy quark FFs are of similar size, which is not too surprising as mass effects are negligible, i.e., $m_{c,b} \ll M_Z$. The gluon-to-eta fragmentation function D_g^η is slightly smaller but rises towards smaller values of z. Overall both the shape and the hierarchy between the different FFs D_i^η is similar to those found, for instance, for pions (see Fig. 18 in [5]) with the exception of the "unfavored" strangeness-to-pion fragmentation function, which is suppressed. In order to make the comparison to FFs for other hadrons more explicit, we show in the lower three rows of Fig. 5 the ratios of the obtained $D_i^\eta(z, M_z)$ to the FFs for pions, kaons, and protons from the DSS analysis [5,6].

The eta and pion production yields are known to be consistent with a constant ratio of about a half in a wide range of c.m.s. energies in hadronic collisions for $p_T \gtrsim 2$ GeV, but the ratio varies from approximately 0.2 at $z \simeq 0.1$ to about 0.5 for $z \gtrsim 0.4$ in SIA [17]. It is interesting to see how these findings are reflected in the ratios of the eta and neutral pion FFs for the individual parton flavors. We find that $D_{u+\bar{u}}^\eta / D_{u+\bar{u}}^{\pi^0}$ follows closely the trend of the SIA data as is expected since gluon fragmentation enters only at NLO in the cross section calculations. For strangeness the rate of eta to pion FFs increases towards larger z because of the absence of strange quarks in the pion wave functions.

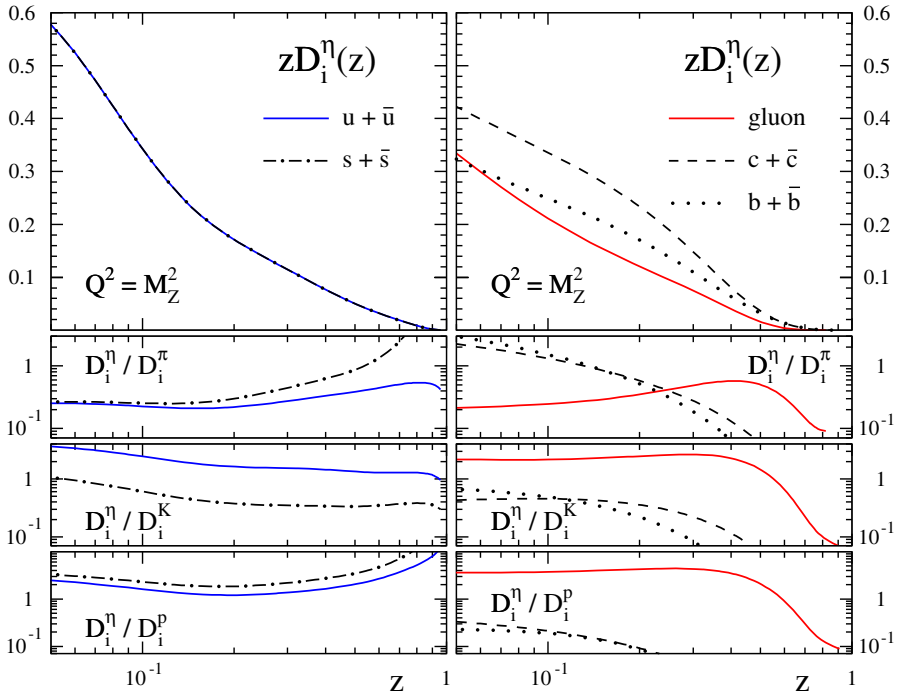

FIG. 5 (color online). Upper panels: Individual FFs for eta mesons $zD_i^\eta(z, Q^2)$ at $Q^2 = M_Z^2$ for $i = u + \bar{u}$, $s + \bar{s}$, g, $c + \bar{c}$, and $b + \bar{b}$. Lower three rows of panels: Ratios of our eta FFs to the ones for pions, kaons, and protons as obtained in the DSS analysis [5,6].

Inclusive hadron production at small-to-medium values of p_T is known to be dominated by gluon fragmentation at relatively large values of momentum fraction z [5,37] largely independent of the c.m.s. energy $\sqrt{S}$. In the relevant range of z, $0.4 \lesssim z \lesssim 0.6$, the ratio $D_g^\eta/D_g^{\pi^0}$ resembles the constant ratio of roughly 0.5 found in the eta-to-pion production yields. At both larger and smaller values of z the D_g^η is suppressed with respect to $D_g^{\pi^0}$. In general, one should keep in mind that FFs always appear in complicated convolution integrals in theoretical cross section calculations [22,23] which complicates any comparison of cross section and fragmentation function ratios for different hadrons.

The comparison to the DSS kaon FFs [5] is shown in the panels in the third row of Fig. 5. Most remarkable is the ratio of the gluon FFs, which is approximately constant, $D_g^\eta/D_g^K \simeq 2$, over a wide region in z but drops below one for $z \gtrsim 0.6$. At large z, $D_{u+\bar{u}}^\eta$ tends to be almost identical to $D_{u+\bar{u}}^K$, while $D_{s+\bar{s}}^\eta$ resembles $D_{s+\bar{s}}^K$ only at low z. The latter result might be understood due to the absence of strangeness suppression for $D_{s+\bar{s}}^K$, whereas a fragmenting s quark needs to pick up an $\bar{s}$ quark from the vacuum to form the eta meson. It should be noted, however, that kaon FFs have considerably larger uncertainties than pion FFs [5] which makes the comparisons less conclusive.

This is even more true for the proton FFs [6]. Nevertheless, it is interesting to compare our D_i^η to those for protons which is done in the lower panels of Fig. 5. As for kaons, we observe a rather flat behavior of the ratio D_g^η/D_g^p, which drops below one at larger values of z. The corresponding rates for light quark FFs show the opposite trend and rise towards $z \to 1$.

Regarding the relative sizes of the fragmentation probabilities for light quarks and gluons into the different hadron species, we find that eta FFs are suppressed with respect to pion FFs (except for strangeness), are roughly similar to those for kaons, and are larger than the proton FFs. This can be qualitatively understood from the hierarchy of the respective hadron masses. For $z \gtrsim 0.6$, the lack of decisive constraints from the data prevents one from drawing any conclusions in this kinematic region.

As we have already discussed in Sec. II A, due to the lack of any flavor-tagged SIA data sensitive to the hadronization of charm and bottom quarks into eta mesons, we adopted the same functional form as for the fragmentation into residual charged hadrons [6], i.e., hadrons other than pions, kaons, and protons. The fit favors a charm fragmentation almost identical to that for the residual hadrons ($N_c = 1.058$) and a somewhat reduced distribution for bottom fragmentation ($N_b = 0.664$). At variance to what is found for light quarks and gluons, after evolution, $D_{c+\bar{c}}^\eta$ and $D_{b+\bar{b}}^\eta$ differ significantly in size and shape from their counterparts for pions, kaons, and protons as can be also inferred from Fig. 5. Future data are clearly needed here for any meaningful comparison.

B. Estimates of uncertainties

Given the relatively small number of data points available for the determination of the D_i^η as compared to global fits of pion, kaon, and proton FFs [5,6], we refrain from performing a full-fledged error analysis. However, in order to get some idea of the uncertainties of the D_i^η associated with experimental errors, how they propagate into observables, and the role of the different data sets in constraining the D_i^η, we perform a brief study based on Lagrange multipliers [5,10,14].

This method relates the range of variation of a physical observable $\mathcal{O}$ dependent on FFs to the variation in the χ^2 function used to judge the goodness of the fit. To this end, one minimizes the function

$$\Phi(\lambda, \{a_i\}) = \chi^2(\{a_i\}) + \lambda \mathcal{O}(\{a_i\}) \tag{4}$$

with respect to the set of parameters $\{a_i\}$ describing the FFs in Eqs. (1) and (2) for fixed values of λ. Each of the Lagrange multipliers λ is related to an observable $\mathcal{O}(\{a_i\})$, and the choice $\lambda = 0$ corresponds to the optimum global fit. From a series of fits for different values of λ one can map out the χ^2 profile for any observable $\mathcal{O}(\{a_i\})$ free of the assumptions made in the traditional Hessian approach [41].

As a first example and following the DSS analyses [5,6], we discuss the range of variation of the truncated second moments of the eta FFs,

$$\xi_i^\eta(z_{\min}, Q) \equiv \int_{z_{\min}}^1 z D_i^\eta(z, Q) dz, \tag{5}$$

for $z_{\min} = 0.2$ and $Q = 5$ GeV around the values obtained in the optimum fit to data, ξ_{i0}^η. In a LO approximation, the second moments $\int_0^1 z D_i^\eta(z, Q) dz$ represent the energy fraction of the parent parton of flavor i taken by the eta meson at a scale Q. The truncated moments in Eq. (5) discard the low-z contributions, which are not constrained by data and, more importantly, where the framework of FFs does not apply. In general, FFs enter calculations of cross sections as convolutions over a wide range of z, and, consequently, the $\xi_i^\eta(z_{\min}, Q)$ give a first, rough idea of how uncertainties in the FFs will propagate to observables.

The solid lines in Fig. 6 show the $\xi_i^\eta(z_{\min}, Q)$ defined in Eq. (5) for $i = u + \bar{u}$, g, $c + \bar{c}$, and $b + \bar{b}$ against the corresponding increase $\Delta\chi^2$ in the total χ^2 of the fit. The two horizontal lines indicate a $\Delta\chi^2$ of one unit and an increase by 2% which amounts to about 4 units in χ^2; see Table II. The latter $\Delta\chi^2$ should give a more faithful estimate of the relevant uncertainties in global QCD analyses [5,6,10,12] than an increase by one unit.

As can be seen, the truncated moment $\xi_{u+\bar{u}}^\eta$, associated with light quark FFs $D_{u+\bar{u}}^\eta = D_{d+\bar{d}}^\eta = D_{s+\bar{s}}^\eta$, is constrained within a range of variation of approximately $^{+30\%}_{-20\%}$ around the value computed with the best fit, assuming a conservative increase in χ^2 by 2%. The estimated uncertainties are considerably larger than the corresponding ones found for

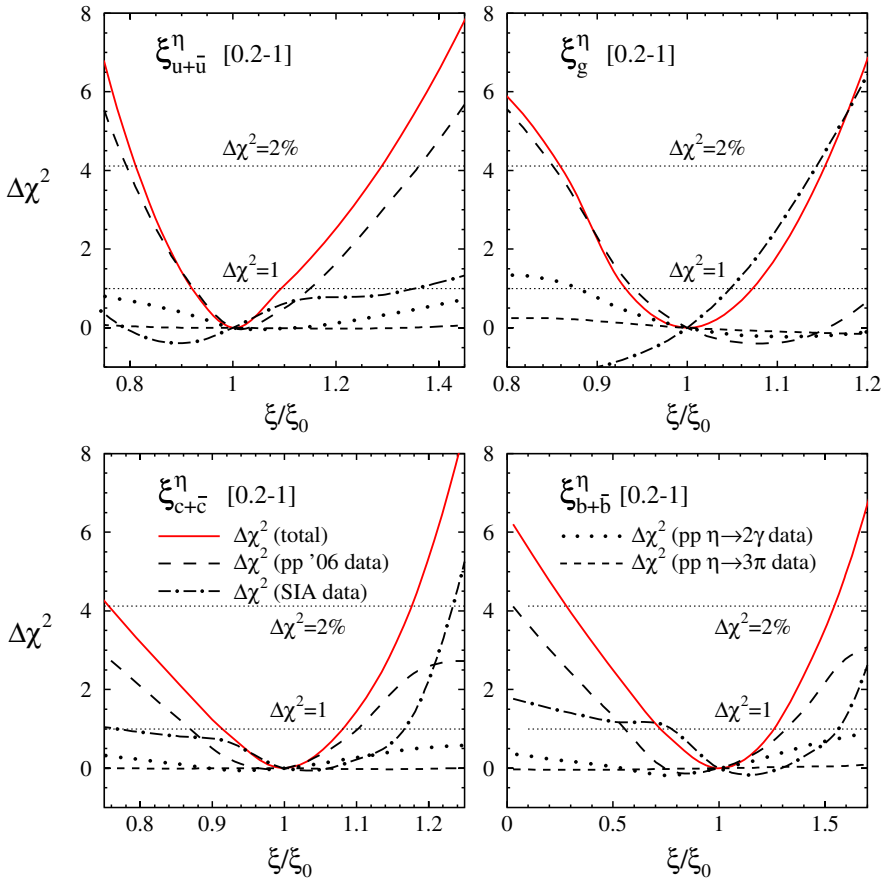

FIG. 6 (color online). Profiles of χ^2 for the NLO eta fragmentation fit as a function of the truncated second moments $\xi_i^{\eta}(z_{\min} = 0.2, Q = 5\ \text{GeV})$ for different flavors (solid lines). In each case, the moments are normalized to the value ξ_0 they take in the best fit to the data. The other lines indicate the partial contributions to $\Delta\chi^2$ of the individual data sets used in the fit.

pion and kaon FFs, which are typically of the order of $\pm 3\%$ and $\pm 10\%$ for the light quark flavors [5], respectively, but closer to the $\pm 20\%$ observed for proton and antiproton FFs [6]. For the truncated moment ξ_g^{η} of gluons shown in the upper right panel of Fig. 6, the range of uncertainty is slightly smaller than the one found for light quarks and amounts to about $\pm 15\%$. The allowed variations are larger for charm and bottom FFs as can be inferred from the lower row of plots in Fig. 6.

Apart from larger experimental uncertainties and the much smaller amount of SIA data for identified eta mesons, the lack of any information from SIDIS is particularly responsible for the large range of variations found for the light quarks in Fig. 6. We recall that the missing SIDIS data for produced eta mesons also forced us to assume that all light quark FFs are the same in Eq. (1). The additional ambiguities due to this assumption are not reflected in the χ^2 profiles shown in Fig. 6.

It is worthwhile mentioning that the only effect we find in the fit when introducing independent FFs for each light quark flavor is the possibility of shifting contributions between them but always preserving the size of their sum, which is what is actually constrained by the data. This additional flexibility at the expense of several additional parameters neither improves the quality of the fit nor increases the error estimate for the total light flavor FF. Nevertheless, in this respect it is important to keep in mind that the quoted uncertainties for any individual light flavor FF are obtained under the assumption of equal FFs: $D^{\eta}_{u+\bar{u}} = D^{\eta}_{d+\bar{d}} = D^{\eta}_{s+\bar{s}}$.

The FFs for charm and bottom quarks into eta mesons suffer most from the lack of flavor-tagged data in SIA. As we have already mentioned in Sec. II, the present data are not able to fully determine the shape of the charm and bottom FFs. Thus, we assume the functional form of the fragmentation into residual hadrons in [6] but allowing for a free normalization. We have checked that different choices have a marginal impact on the best fit and even less on its variations from which we estimate uncertainties.

To further illuminate the role of the different data sets in constraining the D_i^{η} we give also the partial contributions to $\Delta\chi^2$ of the individual data sets from pp collisions and the combined SIA data in all panels of Fig. 6. Surprisingly, the light quark FFs are constrained best by the PHENIX pp data from run '06 and not by SIA data. SIA data alone

would prefer a smaller value for $\xi^{\eta}_{u+\bar{u}}$ by about 10%, strongly correlated to larger moments for charm and bottom fragmentation, but the minimum in the χ^2 profile is much less pronounced and very shallow, resulting in rather sizable uncertainties.

This unexpected result is most likely due to the fact that the SIA data from LEP experiments constrain mainly the flavor singlet combination, i.e., the sum of all quark flavors, including charm and bottom. Since there are no flavor-tagged data available from SIA for eta mesons, the separation into contributions from light and heavy quark FFs is largely unconstrained by SIA data. Only the fairly precise data from *BABAR* at $\sqrt{S} \simeq 10$ GeV provide some guidance as they constrain a different combination of the light u, d, and s quark FFs weighted by the respective electric charges. Altogether, this seems to have a negative impact on the constraining power of the SIA data. For not too large values of p_T, data obtained in pp collisions are in turn mainly sensitive to D^{η}_{g} but in a limited range of z, $0.4 \lesssim z \lesssim 0.6$, as mentioned above. Through the scale evolution, which couples quark and gluon FFs, these data provide a constraint on $\xi^{\eta}_{u+\bar{u}}$. In addition, the latest PHENIX data extend to a region of p_T where quark fragmentation becomes important as well. To illustrate this quantitatively, Fig. 7 shows the relative fractions of quarks and gluons fragmenting into the observed eta meson as a function of p_T in pp collisions for PHENIX kinematics. As can be seen, quark-to-eta FFs become dominant for $p_T \gtrsim 10$ GeV.

The χ^2 profile for the truncated moment of the gluon, ξ^{η}_{g}, is the result of an interplay between the PHENIX run '06 pp data and the SIA data sets which constrain the moment ξ^{η}_{g} towards smaller and larger values, respectively. This highlights the complementarity of the pp and SIA data. SIA data have an impact on ξ^{η}_{g} mainly through the scale evolution in the energy range from LEP to *BABAR*. In addition, SIA data provide information in the entire range of z, whereas the pp data constrain only the large z part of the truncated moment ξ^{η}_{g}. Consequently, the corresponding χ^2 profile for $z_{\min} = 0.4$ or 0.5 would be much more dominated by pp data. In general, the other data sets from PHENIX [17] do not have a significant impact on any of the truncated moments shown in Fig. 6 due to their limited precision and covered kinematic range.

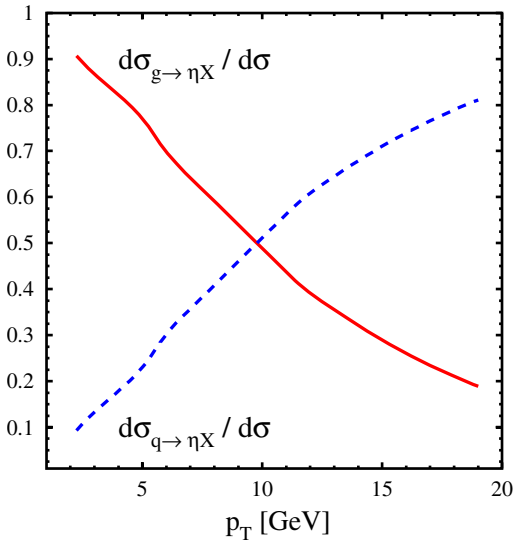

FIG. 7 (color online). Relative fractions of quarks and gluons fragmenting into observed eta meson in pp collisions at $\sqrt{S} = 200$ GeV and PHENIX kinematics [18].

Compared to pion and kaon FFs [5], all χ^2 profiles in Fig. 6 are significantly less parabolic, which prevents one from using the Hessian method [41] for estimating uncertainties. More importantly, the shapes of the χ^2 profiles reflect the very limited experimental information presently available to extract eta FFs for all flavors reliably. Another indication in that direction is provided by the different preferred minima for the values of the ξ^{η}_{i} by the SIA and pp data, although tolerable within the large uncertainties. Our fit is still partially driven by the set of assumptions on the functional form of and relations among different FFs, which we are forced to impose in order to keep the number of free fit parameters at a level such that they can be actually determined by data. Future measurements of eta production in SIA, pp collisions, and, in particular, SIDIS are clearly needed to test the assumptions made in our analysis and to further constrain the D^{η}_{i}.

The large variations found for the individual FFs in Fig. 6 are strongly correlated, and, therefore, their impact on uncertainty estimates might be significantly reduced for certain observables. If, in addition, the observable of interest is only sensitive to a limited range of hadron momentum fractions z, then the corresponding χ^2 profile may assume a more parabolic shape.

In order to illustrate this for a specific example, we compute the χ^2 profiles related to variations in the theoretical estimates of the single-inclusive production of eta mesons in pp collisions at PHENIX kinematics [18]. The results are shown in Fig. 8 for four different values of p_T along with the individual contributions to $\Delta\chi^2$ from the SIA and pp data sets. As anticipated, we find a rather different picture as compared to Fig. 6, with variations only ranging from 5% to 10% depending on the p_T value and tolerating $\Delta\chi^2/\chi^2 = 2\%$. The corresponding uncertainty bands are also plotted in Fig. 4 above for both $\Delta\chi^2 = 1$ and $\Delta\chi^2/\chi^2 = 2\%$ and have been obtained for the other pp data from PHENIX [17] shown in Figs. 2 and 3 as well.

The uncertainties for $pp \to \eta X$ are smallest for intermediate p_T values, where the latest PHENIX measurement [18] is most precise and the three data sets [17,18] have maximum overlap, and increase towards either end of the p_T range of the run '06 data. In particular, at intermediate p_T values, the main constraint comes from the PHENIX run '06 data, whereas SIA data become increasingly

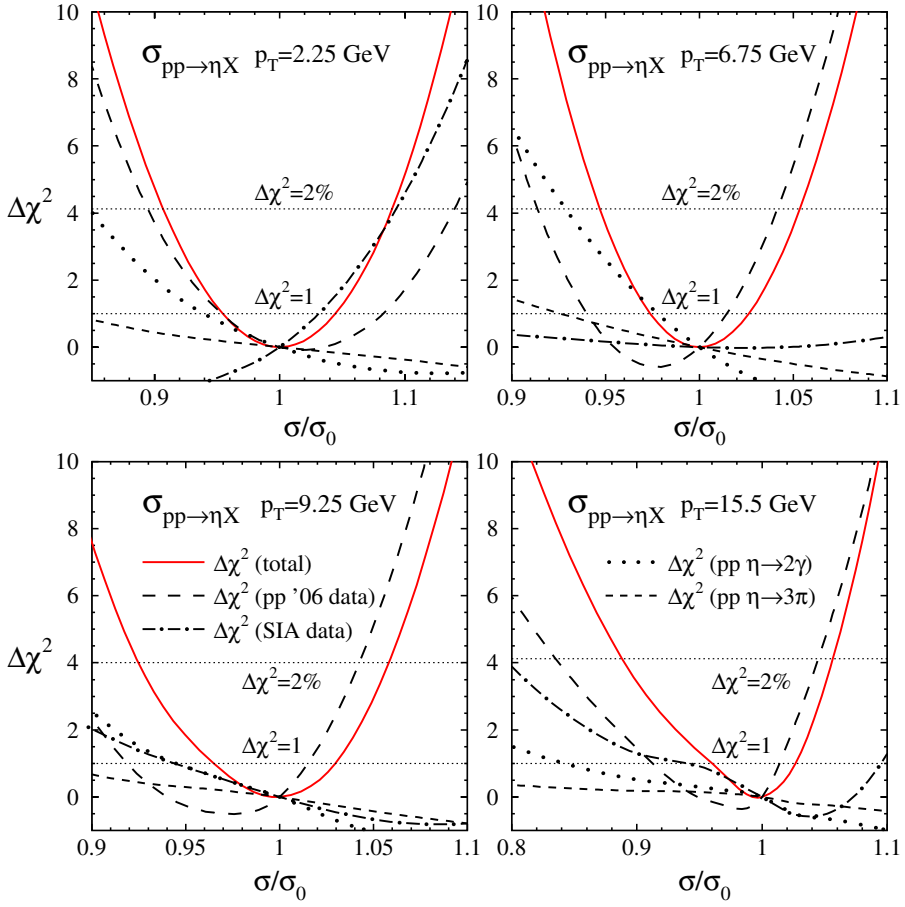

FIG. 8 (color online). As in Fig. 6 but now as a function of the cross section for $pp \to \eta X$ at different values of p_T. The variations of the cross sections are normalized to the value σ_0 obtained in the optimum fit to data.

relevant at low p_T. The previous pp measurements from PHENIX [17] are limited to $p_T \lesssim 11$ GeV and have considerably larger uncertainties and, hence, less impact on the fit.

IV. CONCLUSIONS

A first global QCD analysis of eta fragmentation functions at NLO accuracy has been presented based on the world data from electron-positron annihilation experiments and latest results from proton-proton collisions. The obtained parameterizations [40] reproduce all data sets very well over a wide kinematic range.

Even though the constraints imposed on the eta meson fragmentation functions by presently available data are significantly weaker than those for pions or kaons, the availability of eta FFs extends the applicability of the pQCD framework to new observables of topical interest. Among them are the double-spin asymmetry for eta production in longitudinally polarized proton-proton collisions at RHIC, eta meson production at the LHC, possible medium modifications in the hadronization in the presence of a heavy nucleus, and predictions for future semi-inclusive lepton-nucleon scattering experiments.

The obtained FFs still depend on certain assumptions, like $SU(3)$ symmetry for the light quarks, dictated by the lack of data constraining the flavor separation sufficiently well. Compared to FFs for other hadrons they show interesting patterns of similarities and differences which can be further tested with future data.

ACKNOWLEDGMENTS

We are grateful to David R. Muller for help with the *BABAR* data. C. A. A. gratefully acknowledges the support of the U.S. Department of Energy for this work through the LANL/LDRD Program. The work of F. E. and J. P. S. was supported by Grants No. DE-FG02-04ER41301 and No. DE-FG02-94ER40818, respectively. This work was supported in part by CONICET, ANPCyT, UBACyT, BMBF, and the Helmholtz Foundation.

[1] J. C. Collins and D. E. Soper, Nucl. Phys. **B193**, 381 (1981); **B213**, 545(E) (1983); **B194**, 445 (1982).

[2] See, e.g., J. C. Collins, D. E. Soper, and G. Sterman, in *Perturbative QCD*, edited by A. H. Mueller [Adv. Ser. Direct. High Energy Phys. 5, 1 (1988)], and references therein.

[3] See, e.g., S. Albino, Rev. Mod. Phys. **82**, 2489 (2010); F. Arleo, Eur. Phys. J. C **61**, 603 (2009), and references therein.

[4] R. D. Field and R. P. Feynman, Nucl. Phys. **B136**, 1 (1978).

[5] D. de Florian, R. Sassot, and M. Stratmann, Phys. Rev. D **75**, 114010 (2007).

[6] D. de Florian, R. Sassot, and M. Stratmann, Phys. Rev. D **76**, 074033 (2007).

[7] S. Albino, B. A. Kniehl, and G. Kramer, Nucl. Phys. **B803**, 42 (2008).

[8] M. Hirai, S. Kumano, and T. H. Nagai, Phys. Rev. C **76**, 065207 (2007).

[9] S. Kretzer, Phys. Rev. D **62**, 054001 (2000).

[10] D. de Florian, R. Sassot, M. Stratmann, and W. Vogelsang, Phys. Rev. Lett. **101**, 072001 (2008); Phys. Rev. D **80**, 034030 (2009).

[11] D. de Florian, M. Stratmann, and W. Vogelsang, Phys. Rev. D **57**, 5811 (1998).

[12] P. M. Nadolsky *et al.*, Phys. Rev. D **78**, 013004 (2008).

[13] A. D. Martin, W. J. Stirling, R. S. Thorne, and G. Watt, Eur. Phys. J. C **63**, 189 (2009); R. D. Ball *et al.*, Nucl. Phys. **B838**, 136 (2010).

[14] D. Stump *et al.*, Phys. Rev. D **65**, 014012 (2001).

[15] M. Greco and S. Rolli, Z. Phys. C **60**, 169 (1993).

[16] D. Indumathi, H. S. Mani, and A. Rastogi, Phys. Rev. D **58**, 094014 (1998); D. Indumathi and B. Misra, arXiv:0901.0228.

[17] S. S. Adler *et al.* (PHENIX Collaboration), Phys. Rev. C **75**, 024909 (2007).

[18] A. Adare *et al.* (PHENIX Collaboration), this issue, Phys. Rev. D **83**, 032001 (2011).

[19] See, e.g., A. Accardi, F. Arleo, W. K. Brooks, D. D'Enterria, and V. Muccifora, Riv. Nuovo Cimento Soc. Ital. Fis. **032**, 439 (2010).

[20] R. Sassot, M. Stratmann, and P. Zurita, Phys. Rev. D **81**, 054001 (2010).

[21] G. Curci, W. Furmanski, and R. Petronzio, Nucl. Phys. **B175**, 27 (1980); W. Furmanski and R. Petronzio, Phys. Lett. **97B**, 437 (1980); L. Beaulieu, E. G. Floratos, and C. Kounnas, Nucl. Phys. **B166**, 321 (1980); P. J. Rijken and W. L. van Neerven, Nucl. Phys. **B487**, 233 (1997); M. Stratmann and W. Vogelsang, Nucl. Phys. **B496**, 41 (1997); A. Mitov and S. Moch, Nucl. Phys. **B751**, 18 (2006); A. Mitov, S. Moch, and A. Vogt, Phys. Lett. B **638**, 61 (2006); S. Moch and A. Vogt, Phys. Lett. B **659**, 290 (2008).

[22] G. Altarelli, R. K. Ellis, G. Martinelli, and S. Y. Pi, Nucl. Phys. **B160**, 301 (1979); W. Furmanski and R. Petronzio, Z. Phys. C **11**, 293 (1982); P. Nason and B. R. Webber, Nucl. Phys. **B421**, 473 (1994); **B480**, 755(E) (1996).

[23] F. Aversa, P. Chiappetta, M. Greco, and J. P. Guillet, Nucl. Phys. **B327**, 105 (1989); D. de Florian, Phys. Rev. D **67**, 054004 (2003); B. Jäger, A. Schäfer, M. Stratmann, and W. Vogelsang, Phys. Rev. D **67**, 054005 (2003).

[24] M. Stratmann and W. Vogelsang, Phys. Rev. D **64**, 114007 (2001).

[25] S. Abachi *et al.* (HRS Collaboration), Phys. Lett. B **205**, 111 (1988).

[26] G. Wormser *et al.* (MARK-II Collaboration), Phys. Rev. Lett. **61**, 1057 (1988).

[27] W. Bartel *et al.* (JADE Collaboration), Z. Phys. C **28**, 343 (1985).

[28] D. Pitzl *et al.* (JADE Collaboration), Z. Phys. C **46**, 1 (1990);**47**, 676(E) (1990).

[29] H. J. Behrend *et al.* (CELLO Collaboration), Z. Phys. C **47**, 1 (1990).

[30] D. Buskulic *et al.* (ALEPH Collaboration), Phys. Lett. B **292**, 210 (1992).

[31] R. Barate *et al.* (ALEPH Collaboration), Eur. Phys. J. C **16**, 613 (2000).

[32] A. Heister *et al.* (ALEPH Collaboration), Phys. Lett. B **528**, 19 (2002).

[33] O. Adriani *et al.* (L3 Collaboration), Phys. Lett. B **286**, 403 (1992).

[34] M. Acciarri *et al.* (L3 Collaboration), Phys. Lett. B **328**, 223 (1994).

[35] K. Ackerstaff *et al.* (OPAL Collaboration), Eur. Phys. J. C **5**, 411 (1998).

[36] F. Anulli *et al.* (*BABAR* Collaboration), arXiv:hep-ex/0406017.

[37] R. Sassot, M. Stratmann, and P. Zurita, Phys. Rev. D **82**, 074011 (2010).

[38] L. Apanasevich *et al.* (Fermilab E706 Collaboration), Phys. Rev. D **68**, 052001 (2003).

[39] D. de Florian and W. Vogelsang, Phys. Rev. D **71**, 114004 (2005).

[40] A FORTRAN package containing our NLO set of eta FFs can be obtained upon request from the authors.

[41] P. M. Nadolsky *et al.*, Phys. Rev. D **78**, 013004 (2008).